

## Aerobic Inactivation of *Rhizobium meliloti* NifA in *Escherichia coli* Is Mediated by *lon* and Two Newly Identified Genes, *snoB* and *snoC*

EVA HUALA,† ANNE L. MOON,‡ AND FREDERICK M. AUSUBEL\*

Department of Genetics, Harvard Medical School, and Department of Molecular Biology, Massachusetts General Hospital, Boston, Massachusetts 02114

Received 16 July 1990/Accepted 12 October 1990

The *Rhizobium meliloti* NifA protein is an oxygen-sensitive transcriptional regulator of nitrogen fixation genes. Regulation of NifA activity by oxygen occurs at the transcriptional level through *fixLJ* and at the posttranslational level through the sensitivity of NifA to oxygen. We have previously reported that the NifA protein is sensitive to oxygen in *Escherichia coli* as well as in *R. meliloti*. To investigate whether the posttranslational regulation of NifA is dependent on host factors conserved between *R. meliloti* and *E. coli*, we carried out a Tn5 mutagenesis of *E. coli* and isolated mutants with increased NifA activity under aerobic conditions. Fifteen insertion mutations occurred at three unlinked loci. One locus is the previously characterized *lon* gene; the other two loci, which we have named *snoB* and *snoC*, define previously uncharacterized *E. coli* genes. The products of *snoC* and *lon* affect the rate of NifA degradation, whereas the product of *snoB* may affect both NifA degradation and inactivation. A *snoB lon* double mutant showed a higher level of NifA accumulation than did a *lon* mutant, suggesting that the *snoB* product affects the ability of NifA to be degraded by a *lon*-independent pathway. The effects of a *snoC* mutation and a *lon* mutation were not additive, suggesting that the *snoC* and *lon* products function in the same degradative pathway.

Nitrogen fixation in *Rhizobium meliloti* and other diazotrophs is an inherently oxygen sensitive process. Production of nitrogenase in the presence of oxygen is effectively prevented, since NifA, the transcriptional activator of the nitrogenase structural genes, is regulated at two levels by oxygen. First, the environmental sensor-regulator pair *fixLJ* stimulates *nifA* transcription only under microaerobic conditions (9, 11). Second, the *nifA* gene product (NifA) is itself inactive under aerobic conditions (2, 14, 15). Inactivation of *R. meliloti* NifA under aerobic conditions also occurs when NifA is expressed in *Escherichia coli*, suggesting either that NifA inactivation by oxygen does not require the presence of any host factors or that such factors are present in both *R. meliloti* and *E. coli*. In contrast to the NifA of *R. meliloti*, NifA from the free-living diazotroph *Klebsiella pneumoniae* is oxygen sensitive only in the presence of *nifL*, which is cotranscribed with *nifA* in *K. pneumoniae* but for which no homolog has been found in any symbiotic nitrogen-fixing species. How the *nifL* product modulates NifA activity in *K. pneumoniae* in response to the oxygen level remains unclear.

Previous work on *R. meliloti* NifA demonstrated that small changes in the amino acid sequence of the amino terminus can have a profound effect on the level of NifA accumulation when NifA is expressed in *E. coli* (15). NifA translated from the first in-frame AUG codon (NifA-AUG1) accumulates to very low levels when cells are grown aerobically and reaches slightly higher levels when cells are grown under 1% oxygen. In contrast, several variant NifA proteins with altered amino-terminal sequences accumulate

to very high levels in *E. coli* during aerobic or microaerobic growth, most likely due to differences in stability (15). It appears that these differences in the stability of NifA proteins are mediated by a factor present in *E. coli* but absent in *R. meliloti*, since in *R. meliloti* no difference in accumulation between different forms of NifA was observed (15). To identify factors in *E. coli* that decrease NifA transcriptional activity in the presence of oxygen, we performed a Tn5 mutagenesis of *E. coli* and isolated mutants with increased NifA-AUG1 activity during aerobic growth.

### MATERIALS AND METHODS

**Bacterial strains and media.** The bacterial strains and plasmids used in this study are listed in Table 1. LB medium (19) and M9 and M63 minimal media (20) have been previously described. For selection of kanamycin resistant recipients after P1 transduction, 100 µg of kanamycin per ml was used for streptomycin-resistant strains and 50 µg of kanamycin per ml was used for streptomycin-sensitive strains. In other experiments, antibiotic concentrations were 10 µg/ml for tetracycline, 25 µg/ml for kanamycin, 20 µg/ml for streptomycin, 25 µg/ml for chloramphenicol, and 100 µg/ml for ampicillin.

**Isolation of Tn5 mutants.** MC1061 containing plasmids pEH32 and pMB210 was grown in LB medium to a density of 10<sup>9</sup> cells per ml and infected with λ b221 *rex::Tn5* cI857 *Oam8 Pam29* (1, 24) at a multiplicity of infection of 0.1, incubated at 32°C for 4 h, and plated on M9 minimal medium supplemented with 0.4% lactose as the sole carbon source and 25 µg of kanamycin per ml. Extremely small kanamycin-resistant colonies were visible under a dissecting microscope after 84 h of incubation at 28°C (a temperature that permits high NifA activity) at a density of about 12,000 colonies on each of 16 plates. In addition to these numerous microcolonies, each plate contained from one to eight significantly

\* Corresponding author.

† Present address: Department of Plant Biology, University of California, Berkeley, CA 94720.

‡ Present address: Department of Molecular and Cell Biology, University of California, Berkeley, CA 94720.

TABLE 1. Bacterial strains and plasmids

Strain or plasmid	Relevant characteristics	Source or reference
<i>E. coli</i>		
MC1061	<i>araD139 Δ(ara leu)7697 ΔlacX74 galU galK hsr hsm strA</i>	6
Mph82	<i>lon::Tn10</i> (SW7J2B)	5
HA62	MC1061 with <i>lon::Tn10</i> from Mph82	This work
HA63	LC23 with <i>lon::Tn10</i> from Mph82	This work
HA64	LC24 with <i>lon::Tn10</i> from Mph82	This work
LC12	Tn5 mutant of MC1061 ( <i>snoA</i> )	This work
LC4	Tn5 mutant of MC1061 ( <i>snoB</i> )	This work
LC6	Tn5 mutant of MC1061 ( <i>snoB</i> )	This work
LC23	Tn5 mutant of MC1061 ( <i>snoB</i> )	This work
LC25	Tn5 mutant of MC1061 ( <i>snoB</i> )	This work
LC24	Tn5 mutant of MC1061 ( <i>snoC</i> )	This work
C-1A	Prototroph	26
LC241A	C-1A containing LC24 Tn5	This work
BW6160	Hfr:: <i>Tn10</i>	30
BW7620	Hfr:: <i>Tn10</i>	30
BW5660	Hfr:: <i>Tn10</i>	30
BW6175	Hfr:: <i>Tn10</i>	30
BW6164	Hfr:: <i>Tn10</i>	30
NK6051	Hfr:: <i>Tn10</i>	30
BW6165	Hfr:: <i>Tn10</i>	30
BW6156	Hfr:: <i>Tn10</i>	30
BW7261	Hfr:: <i>Tn10</i>	30
BW7623	Hfr:: <i>Tn10</i>	30
BW7622	Hfr:: <i>Tn10</i>	30
BW5659	Hfr:: <i>Tn10</i>	30
BW6163	Hfr:: <i>Tn10</i>	30
BW6169	Hfr:: <i>Tn10</i>	30
BW6166	Hfr:: <i>Tn10</i>	30
CAG12169	<i>zch-506::Tn10</i>	28
CAG12028	<i>zci-233::Tn10</i>	28
CAG12081	<i>zci-3061::Tn10</i>	28
CAG12026	<i>trg-2::Tn10</i>	28
Plasmids		
pSDC13	M13 <i>ori</i> , <i>ColE1 ori</i> , <i>Cm<sup>r</sup></i>	18
pEH32	pSDC13 with <i>lacZ-nifA</i> (NifA-AUG1)	15
pEHΔR1	pSDC13 with <i>lacZ-nifA</i> (NifA-ΔN)	15
pMB210	<i>nifH-lacZ</i> , <i>RK2 ori</i> , <i>Tc<sup>r</sup></i>	2
pLAC	<i>lacZ</i> , <i>RK2 ori</i> , <i>Tc<sup>r</sup></i>	15

larger colonies. Of a total of about 90 large colonies, 21 were purified by streaking on lactose minimal plates plus kanamycin. Several of the kanamycin-resistant microcolonies were also purified to serve as controls.

**Genetic techniques and physical mapping.** Transduction of Tn5 insertions by P1vir was carried out as previously described (20), except recipient strains were diluted 1:20 from a fresh overnight culture and grown at 37°C for 2 h before the transducing lysate was added. Hfr mapping was carried out as previously described (30) with a set of Hfr::*Tn10* strains kindly supplied by B. Bachman (Table 1). The physical map location of the LC24 Tn5 insertion was obtained by Southern blot analysis (8). MC1061 DNA digested separately with *Bam*HI, *Hind*III, *Eco*RI, *Eco*RV, *Bgl*II, *Kpn*I, *Pst*I, or *Pvu*II was probed with flanking DNA from the LC24 insertion, and the resulting restriction patterns were compared with the physical map of the *E. coli* genome generated by Kohara et al. (16).

**β-Galactosidase assays.** Bacterial strains containing a *lacZ-nifA*-expressing plasmid (pEH32 or pEHΔR1) and a *nifH-lacZ* reporter plasmid (pMB210) were grown in LB medium

plus antibiotics at 28°C under a continuous stream of 1% oxygen or 21% oxygen as previously described (15). The amount of active NifA present after 16 h of growth was measured by assaying the cultures for β-galactosidase activity (20).

**Immunological techniques.** Antibodies were prepared against a peptide containing the last 14 amino acids of *R. meliloti* NifA (NH<sub>3</sub>-Gly-Tyr-Ala-Leu-Arg-Arg-His-Gly-Val-Asp-Val-Arg-Lys-Leu-COOH) kindly synthesized by John Smith, Department of Molecular Biology, Massachusetts General Hospital. The peptide was conjugated by using *m*-maleimidobenzoyl-*N*-hydroxysuccinimide ester (Pierce) to the carrier protein keyhole limpet hemocyanin (Sigma) through an extra cysteine residue added at the amino terminus of the peptide. The carrier protein (10 mg) was dissolved in 0.7 ml of 1 M potassium phosphate buffer (pH 7.3) and diluted to 7 ml in deionized water. *m*-Maleimidobenzoyl-*N*-hydroxysuccinimide ester (6 mg) was dissolved in 100 μl of 50% dimethyl formamide–50% tetrahydrofuran and added dropwise to the carrier protein with constant stirring. After 6 mg of the synthetic peptide was added, the reaction was stirred at room temperature overnight and then dialyzed for 24 h against 4 liters of phosphate-buffered saline. Immunization of two New Zealand Red rabbits was carried out subcutaneously with 0.67 ml of conjugated peptide emulsified with 0.33 ml of Freund complete adjuvant (Calbiochem) followed by two boosts, with 0.5 ml of conjugated peptide and 0.5 ml of Freund incomplete adjuvant, at 16 and 31 days after the initial injections.

Western immunoblots were performed as previously described (3) with alkaline phosphatase-conjugated goat anti-rabbit immunoglobulin G (Calbiochem) as the secondary antibody. Nitro Blue Tetrazolium and 5-bromo-4-chloro-3-indolyl phosphate for the alkaline phosphatase reaction were from Sigma.

**Pulse-chase and immunoprecipitation.** Cultures containing pEHΔR1 were grown overnight in LB medium, diluted 1:100 in M9 medium plus 0.5% glycerol, 40 μg of L-amino acids except methionine and cysteine per ml, 0.5 mg of thiamine per liter, and antibiotics, and then grown aerobically in an environmental shaker at 37°C for several hours. When the optical density of the culture at 600 nm reached a level between 0.1 and 0.5, the cultures were diluted to an optical density of 0.1 in the same medium and grown at 28°C for 2 h in an environmental shaker. The cultures were pulse-labeled by the addition of 37.5 μCi of L-[<sup>35</sup>S]methionine (1245 Ci/mmol; New England Nuclear) per ml; after 2 min excess unlabeled L-methionine was added to a final concentration of 1.4 mg/ml (21), and the culture was maintained at 28°C throughout the chase period. At intervals, 0.5-ml aliquots were added to 35 μl of 60 mM phenylmethylsulfonyl fluoride and 80 mM sodium azide in 90% ethanol on ice. Labeled cells were collected by centrifugation, suspended in 30 μl of sodium dodecyl sulfate (SDS) sample buffer (125 mM Tris [pH 6.8], 5 mM EDTA, 10% glycerol, 5% β-mercaptoethanol, 2% SDS), and boiled for 5 min.

Immunoprecipitation of pulse-labeled samples was carried out by adding 10 to 30 μl of the boiling lysate to 970 μl of phosphate-buffered saline and 5 μl of antiserum, agitating overnight at 22°C, and precipitating the bound antibodies with protein A-Sepharose (Pharmacia) as previously described (29). NifA protein was released from the washed protein A-Sepharose pellet by boiling in SDS sample buffer for 5 min, and the samples were electrophoresed on a 10% polyacrylamide–SDS gel.

The amount of radioactivity present in the NifA bands

resulting from the pulse-chase experiment was measured with a Betascope 603 blot analyzer (Betagen). Least-squares regression analysis was used to determine the half-life for NifA-ΔN.

**Tn5 cloning and sequence analysis.** Chromosomal DNA from mutants LC12, LC23, and LC24 was digested with *EcoRI*, *Sall*, or *BamHI* and ligated into pMLC28. The resulting kanamycin-resistant colonies contained plasmids carrying part or all of the Tn5 insertion and flanking DNA. The DNA adjacent to the Tn5 insertions was sequenced by the dideoxy method (25) with a Sequenase kit (U.S. Biochemical) with a Tn5-specific primer (3'-GTTCATCGCAG GACTTG-5'; 23).

**Growth curves.** It has been previously reported that *E. coli dcp* mutants are incapable of cleaving *N*-acetyl-Ala-Ala-Ala (Sigma) and therefore cannot grow on this compound as the sole nitrogen source (10). To test whether the LC24 Tn5 insertion is located in *dcp*, the Tn5 insertion from LC24 was transduced to a prototrophic *E. coli* strain, C-1A. The resulting strain, LC241A, was grown overnight at 37°C in M63 minimal medium, diluted 1:10 in M63, and grown for several hours until the optical density exceeded 0.05 at 600 nm. Each culture was diluted to an optical density of 0.05 in M63 and then diluted 1:100 in either M63 containing 10 mg of ammonium sulfate per ml or in M63 without ammonium sulfate containing 10 mM *N*-acetyl-Ala-Ala-Ala as the sole nitrogen source; the growth of the cultures was observed by measuring the optical density of the cultures at 600 nm periodically over 24 h.

## RESULTS

**Tn5 mutagenesis and selection of mutants.** *E. coli* MC1061, carrying the *lacZ-nifA* expression plasmid pEH32 and the *nifH-lacZ* reporter plasmid pMB210, was mutagenized with Tn5 and plated on lactose minimal plates; MC1061 carrying these two plasmids grew very poorly on this medium, producing barely visible colonies after 84 h of growth at 28°C. Mutants with an increased level of NifA activity, resulting in an increased ability to activate expression of the *nifH-lacZ* fusion, were expected to appear as larger colonies against a background of microcolonies. Twenty-one large kanamycin-resistant colonies were isolated by restreaking on lactose minimal medium, and their large size was verified by plating each one on lactose minimal medium and comparing them with colonies of wild-type MC1061 carrying pEH32 and pMB210. To determine whether the Tn5 insertions were chromosomal, plasmid DNA was isolated from each mutant and used to transform *E. coli* MC1061. No kanamycin-resistant colonies resulted, indicating that the Tn5 insertions were located on the chromosome.

Total DNA from each mutant strain was prepared, digested with *EcoRI*, and analyzed on a Southern blot with a Tn5 probe. Four mutants carrying more than one Tn5 insertion (LC9, LC11, LC21, LC22) and two mutants with weak phenotypes (LC5, LC18) were not characterized further. The remaining Tn5 insertions occurred in three different *EcoRI* fragments. Group 1 (*snoA*, for stability of NifA in oxygen) consisted of 10 members (LC2, LC3, LC7, LC8, LC10, LC12, LC13, LC14, LC15, LC16), group 2 (*snoB*) consisted of 4 members (LC4, LC6, LC23, LC25), and group 3 (*snoC*) consisted of 1 member (LC24). One representative from each group (LC12, LC23, LC24) was chosen for further characterization. The approximate chromosomal locations of *snoA*, *snoB*, and *snoC* were determined by Hfr mapping to be between 6 and 13 min for *snoA*, between 23 and 30 min for

TABLE 2. NifA activity in wild-type and mutant *E. coli*

Strain	β-Galactosidase activity (Miller units)	
	1% oxygen	21% oxygen
MC1061	7.6	7.9
MC1061(pMB210) <sup>a</sup>	144	169
LC12(pMB210)	99	164
LC23(pMB210)	135	129
LC24(pMB210)	133	183
MC1061(pMB210, pEH32) <sup>b</sup>	46,128	1,367
LC12(pMB210, pEH32)	67,902	12,650
LC23(pMB210, pEH32)	48,789	13,859
LC24(pMB210, pEH32)	60,341	15,163
MC1061(pMB210, pEHΔR1) <sup>c</sup>	53,189	35,836
LC12(pMB210, pEHΔR1)	60,017	42,847
LC23(pMB210, pEHΔR1)	54,584	28,660
LC24(pMB210, pEHΔR1)	57,398	45,205
MC1061(pLAC) <sup>d</sup>	41,420	32,901
LC12(pLAC)	37,615	30,452
LC23(pLAC)	31,538	25,882
LC24(pLAC)	34,133	29,388

<sup>a</sup> pMB210 carries a *nifH-lacZ* reporter fusion.

<sup>b</sup> pEH32 expresses NifA-AUG1 from the *lacZ* promoter.

<sup>c</sup> pEHΔR1 expresses NifA-ΔN from the *lacZ* promoter.

<sup>d</sup> pLAC expresses the *lacZ* gene from its natural promoter.

*snoB*, and between 51 and 61 min for *snoC* (see Materials and Methods; data not shown).

**Mutant phenotypes.** Mutants LC12, LC23, and LC24 containing the plasmids pEH32 (NifA-AUG1) and pMB210 (*nifH-lacZ*) were grown in LB medium under a continuous stream of either 1 or 21% oxygen for 16 h and assayed for β-galactosidase activity from the *nifH-lacZ* reporter fusion. When grown under 21% oxygen, all three mutants showed levels of β-galactosidase activity about 10-fold higher than that of the wild-type strain (MC1061) containing pEH32 and pMB210 (data not shown). At 1% oxygen, LC12 and LC24 showed slightly elevated levels of β-galactosidase activity relative to MC1061, whereas LC23 showed no relative increase in β-galactosidase activity. To confirm that the phenotypes of the mutants were caused by the Tn5 insertions rather than by unlinked mutations, the Tn5 insertions of strains LC12, LC23, and LC24 were transduced into MC1061 by using phage P1. The transductants were transformed with pEH32 and pMB210 and assayed for β-galactosidase activity at 21% oxygen. The transduced strains, like the original mutants, showed a 10-fold-elevated level of β-galactosidase activity relative to MC1061 (Table 2). The increased level of β-galactosidase activity in the mutant strains was fully dependent on the presence of NifA. No increase in the basal level of activity due to constitutive activity of the *nifH* promoter was seen in the absence of NifA in any of the mutants (Table 2).

The effect of the *sno* mutations on a more stable mutant form of NifA carried on plasmid pEHΔR1 was also tested. The NifA protein expressed from this plasmid (NifA-ΔN) carries a deletion of the amino-terminal domain that results in a high level of NifA-ΔN accumulation in *E. coli* (15). Strains LC12, LC23, and LC24 containing pEHΔR1 and pMB210 were tested for β-galactosidase activity at 1 and 21% oxygen (Table 2). NifA-ΔN activity was only slightly

higher in LC12 (*snoA*) and LC24 (*snoC*) than in MC1061, whereas a slight decrease in NifA- $\Delta$ N activity was observed in LC23 (*snoB*).

***snoA* mutations are in *lon*.** Hfr mapping of the *snoA* insertion in LC12 showed that the location of *snoA* was between 6 and 13 min on the *E. coli* genetic map. The location of the insertion of the physical map of Kohara et al. (16) was determined by Southern blot analysis (data not shown) to be about 55 kb from *proC* (the nearest genetic marker on the map of Kohara et al.) in the vicinity of *lon*, which encodes the protease La. The Tn5 insertion and flanking DNA from LC12 was cloned, and about 300 bp on either side of the Tn5 insertion were sequenced (data not shown). Comparison of this sequence with the sequence of the *lon* gene showed that the *snoA* insertion in LC12 is within *lon*. The Tn5 insertion in LC12 follows nucleotide 1038 of the *lon* sequence reported by Chin et al. (7) and has resulted in the duplication of a *Pst*I site located about one-fourth of the way through the *lon* coding region. We did not determine the location of the remaining nine Tn5 insertions located within the approximately 14-kb *Eco*RI fragment carrying *lon*.

**Location of *snoB*.** The Tn5 insertion from LC23 (*snoB*) was cloned, and a 270-bp region of flanking DNA was sequenced (data not shown). A search of the Genbank sequence data base with the sequence of the flanking DNA revealed that the Tn5 insertion in this mutant is located approximately 160 bp downstream of the termination codon for *alaS*, encoding alanyl-tRNA synthetase (22). To confirm that the Tn5 insertions in LC4, LC6, and LC25 were also near *alaS*, we measured the frequency of cotransduction of these Tn5 insertions with an *srlC300::Tn10* insertion from strain BW5660 (30). We tested 7 to 10 transductants for each insertion and found that all four *snoB* Tn5 insertions were cotransduced with *srlC* at frequencies ranging from 86 to 100%. Southern analysis with *Sal*I-restricted DNA from LC4, LC6, LC23, and LC25 showed that two insertions (LC23 and LC6) are located about 400 bp downstream from a *Sal*I site near the 3' end of *alaS* and that the other two insertions (LC4 and LC25) are about 750 bp from this *Sal*I site.

**Location of *snoC*.** We cloned and sequenced 221 bp of flanking DNA from the LC24 (*snoC*) insertion. No matching sequence was found in the Genbank data base. Since the rough location for this insertion has been determined by Hfr mapping to lie in the region of 23 to 31 min of the *E. coli* genetic map, we tested for P1 cotransduction with a series of Tn10 insertions in this region. A Tn10 insertion at 29.3 min (*zcf-3061::Tn10*) was determined to be 84% cotransducible with the LC24 Tn5 insertion. The location of the insertion on the physical map of Kohara et al. (16) was determined by Southern analysis of MC1061 DNA restricted with the eight mapping enzymes used in the generation of the physical map (see Materials and Methods) and probed with the cloned flanking DNA from the LC24 insertion (see Fig. 4). The results of the physical and genetic mapping indicate that the LC24 insertion is located about 10 kb away from *nirR* (29.4 min) in the direction of *rac*. The *dcp* gene, which encodes dipeptidyl carboxypeptidase, maps in this vicinity (10). To determine whether the Tn5 insertion of LC24 falls within *dcp*, we transduced the Tn5 insertion of LC24 into the prototrophic strain C-1A to create strain LC241A and measured the effect of the insertion on the ability of this strain to grow in minimal medium with *N*-acetyl-Ala-Ala-Ala as the sole nitrogen source. Wild-type *E. coli* is capable of growing on this substrate, whereas *dcp* mutants are incapable of

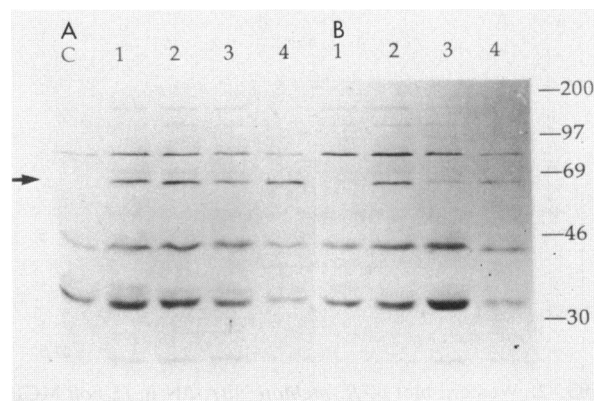


FIG. 1. Western blot of *R. meliloti* NifA-AUG1 in *E. coli* MC1061 and mutant derivatives grown under 1% (A) or 21% (B) oxygen. Lanes: C, MC1061 containing only vector (no NifA); 1, MC1061 with pEH32 (NifA-AUG1); 2, HA62 (*lon*) with pEH32; 3, LC23 (*snoB*) with pEH32; 4, LC24 (*snoC*) with pEH32. The positions of molecular weight markers (in thousands) are shown on the right. The arrow indicates the location of NifA.

cleaving this tripeptide and cannot use it as a nitrogen source (10). Comparison of the growth rates of C-1A and LC241A revealed no difference in the ability of these strains to grow on *N*-acetyl-Ala-Ala-Ala as the sole nitrogen source (data not shown), indicating that the Tn5 insertion in LC24 is probably not in *dcp*. However, this possibility cannot be entirely ruled out until the *dcp* gene from LC24 is demonstrated to complement a known *dcp* mutation. It cannot be assumed that all alleles of *dcp* have an identical phenotype with respect to metabolism of *N*-acetyl-Ala-Ala-Ala.

**Accumulation of NifA protein.** To determine whether an increase in the accumulation of NifA-AUG1 was responsible for the increased level of  $\beta$ -galactosidase activity in the mutants, NifA-AUG1 accumulation in MC1061, HA62 (a *lon::Tn10* derivative of MC1061), LC23 (*snoB*), and LC24 (*snoC*) was compared by Western blot analysis. NifA-AUG1 accumulation with 1% oxygen was about equal in all four strains (Fig. 1A), but the accumulation with 21% oxygen varied. Whereas NifA-AUG1 decreased to an undetectable level in MC1061 grown under 21% oxygen (Fig. 1B, lane 1), NifA-AUG1 in HA62 (*lon*) grown under the same conditions showed no decrease relative to its accumulation under 1% oxygen (Fig. 1B, lane 2). Like HA62 (*lon*), LC24 (*snoC*) consistently showed a noticeable increase in NifA-AUG1 accumulation with 21% oxygen, which is apparent when the intensity of the background bands are compared with the NifA band (Fig. 1B, lane 4) and which was also seen in other experiments. However, only a slight increase in NifA-AUG1 accumulation was seen for LC23 (*snoB*) grown under 21% oxygen (Fig. 1B, lane 3). These results suggest that mutations in *lon*, *snoB*, and *snoC* may cause a decrease in the NifA degradation rate or an increase in the rate of NifA synthesis at high oxygen tension. Although the increase in NifA-AUG1 accumulation was slight in the *snoB* mutant, the effect of this mutation on NifA-AUG1 activity was as strong as that of the *lon* and *snoC* mutations. This suggests that the main effect of a *snoB* mutation may be to increase the activity of NifA-AUG1 under 21% oxygen rather than its rate of accumulation, possibly through a decrease in the rate of NifA-AUG1 inactivation by oxygen.

Although the *sno* mutations did not have any obvious

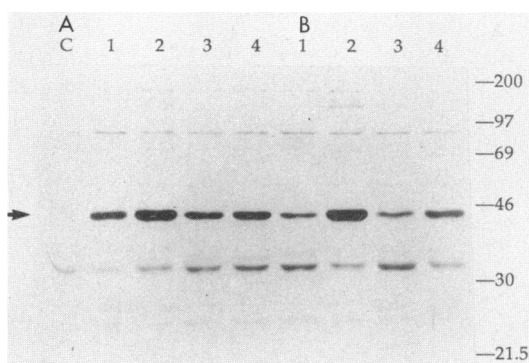


FIG. 2. Western blot of *R. meliloti* NifA- $\Delta$ N in *E. coli* MC1061 and mutant derivatives grown under 1% (A) or 21% (B) oxygen. Lanes: C, MC1061 containing only vector (no NifA); 1, MC1061 with pEH $\Delta$ R1 (NifA- $\Delta$ N); 2, HA62 (*lon*) with pEH $\Delta$ R1; 3, LC23 (*snoB*) with pEH $\Delta$ R1; 4, LC24 (*snoC*) with pEH $\Delta$ R1. The positions of molecular weight markers (in thousands) are shown on the right.

effect on NifA- $\Delta$ N activity, we also compared the accumulation of this mutant form of NifA in MC1061, HA62 (*lon*), LC23 (*snoB*), and LC24 (*snoC*) (Fig. 2). The accumulation of NifA- $\Delta$ N in MC1061 was much higher than accumulation of NifA-AUG1 under both 1 and 21% oxygen, probably because of an increase in protein stability, but accumulation remained lower under 21% oxygen (Fig. 2A, lanes 1) (15). The *lon* mutation (HA62; Fig. 2A, lane 2) caused a visible increase in NifA- $\Delta$ N accumulation even under 1% oxygen and once again prevented any decrease in accumulation under 21% oxygen (Fig. 2B, lane 2). The *snoC* mutation (LC24) also caused a slight increase in NifA- $\Delta$ N accumulation under both 1 and 21% oxygen (Fig. 2, lanes 4), whereas LC23 (*snoB*) showed no increased accumulation of NifA- $\Delta$ N relative to MC1061 (Fig. 2, lanes 3). Overall, the effect of the *sno* mutations on accumulation of NifA-AUG1 and NifA- $\Delta$ N under 21% oxygen was similar, except in the case of the *snoB* mutation, which caused a slight increase in accumulation of NifA-AUG1 but not of NifA- $\Delta$ N.

**Accumulation of NifA in *snoAB* and *SnoAC* double mutants.** The *lon::Tn10* insertion from Mph82 was transduced into

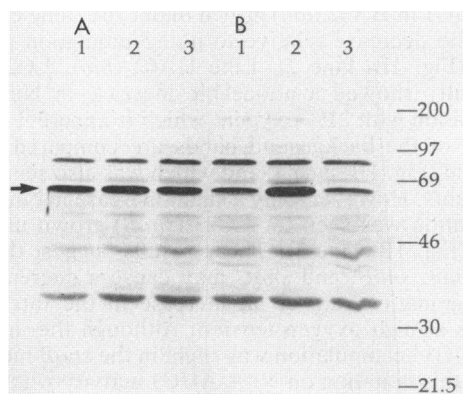


FIG. 3. Western blot of *R. meliloti* NifA-AUG1 in *E. coli* *lon*, *snoB lon*, and *snoC lon* mutants grown under 1% (A) or 21% (B) oxygen. Lanes: 1, HA62 (*lon*) with pEH32 (NifA-AUG1); 2, HA63 (*snoB lon*) with pEH32; 3, HA64 (*snoC lon*) with pEH32. The positions of molecular weight markers (in thousands) are shown on the right.

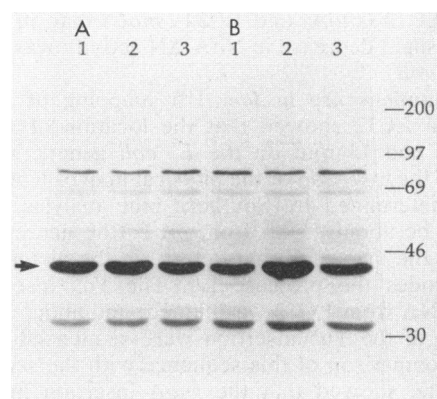


FIG. 4. Western blot of *R. meliloti* NifA- $\Delta$ N1 in *E. coli* *lon*, *snoB lon*, and *snoC lon* mutants grown under 1% (A) or 21% (B) oxygen. Lanes: 1, HA62 (*lon*) with pEH $\Delta$ R1 (NifA- $\Delta$ N); 2, HA63 (*snoB lon*) with pEH $\Delta$ R1; 3, HA64 (*snoC lon*) with pEH $\Delta$ R1. The positions of molecular weight markers (in thousands) are shown on the right.

LC23 and LC24 to create strains HA63 (*lon snoB*) and HA64 (*lon snoC*). These double mutants were transformed with pEH32 or pEH $\Delta$ R1, and the accumulation of NifA was monitored on Western blots (Fig. 3 and 4). HA64 (*lon snoC*; Fig. 3, lane 3) accumulated NifA-AUG1 to the same level as HA62 (*lon*; Fig. 3, lane 1), indicating that the effects of mutations in *snoC* and *lon* are not additive. However, HA63 (*lon snoB*; Fig. 3, lane 2) showed increased accumulation when compared with HA62 (*lon*).

The effect of *lon snoB* and *lon snoC* double mutations on accumulation of NifA- $\Delta$ N was also examined (Fig. 4). Once again, HA64 (*lon snoC*; Fig. 4, lane 3) accumulated NifA- $\Delta$ N to the same level as HA62 (*lon*; Fig. 4, lane 1), whereas HA63 (*lon snoB*; Fig. 4, lane 2) showed increased accumulation when compared with HA62 (*lon*). This result was unexpected, since the *snoB* insertion appeared to have no effect on NifA- $\Delta$ N accumulation by itself (Fig. 1). The effect of the *lon snoC* double mutation on accumulation of both NifA-AUG1 and NifA- $\Delta$ N suggests that the *snoC* gene product acts with the *lon* gene product to decrease the accumulation of NifA, since the NifA level is lowered only when a cell has wild-type copies of both genes. In contrast, the *snoB* mutation somehow caused a decrease in NifA degradation, which in the case of NifA- $\Delta$ N was only apparent in the presence of a *lon* mutation. This could be explained if a decrease in NifA- $\Delta$ N degradation through a Lon-independent pathway in a *snoB* mutant is offset by a compensating increase in Lon-mediated degradation.

***sno* mutations have no effect on the *lac* promoter.** Several explanations are possible for the observed increase in NifA accumulation in LC12 (*snoA*) and LC24 (*snoC*), including increased transcription of *nifA* from the *lac* promoter, an increase in the translation efficiency, or a decrease in the rate of NifA degradation. To test whether transcription from the *lac* promoter is increased in these mutants, the expression of  $\beta$ -galactosidase from a plasmid-borne copy of the *lacZ* gene expressed from its natural promoter (plasmid pLAC) was compared in *E. coli* MC1061, LC12 (*snoA*), LC23 (*snoB*), and LC24 (*snoC*) (Table 2). No difference in  $\beta$ -galactosidase activity was detected in the mutants, suggesting that the activity of the *lac* promoter and *lac* ribosome binding site was not affected by the mutations. The amount of  $\beta$ -galactosidase protein produced from pLAC in MC1061, LC12, LC23, and LC24 was also compared on an SDS-polyacryl-

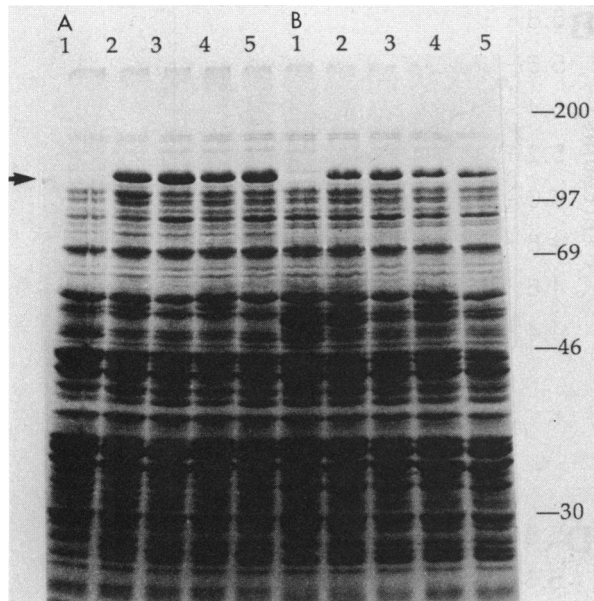


FIG. 5. Expression of  $\beta$ -galactosidase from the *lacZ* promoter: SDS-polyacrylamide gel of total protein of cells grown under 1% (A) or 21% (B) oxygen. Lanes: 1, MC1061 (pMB210); 2, MC1061 (pLAC); 3, LC12 (pLAC); 4, LC23 (pLAC); 5, LC24 (pLAC). The arrow indicates the position of  $\beta$ -galactosidase. The positions of molecular markers (in thousands) are shown on the right.

amide gel. No differences in the level of  $\beta$ -galactosidase in MC1061 and the *sno* mutants were observed after growth under 1 or 21% oxygen (Fig. 5). Since the *lacZ* ribosome binding site and 5'-untranslated sequences are present in both the *lacZ* test plasmid and the *lacZ-nifA* fusion carried on pEH32, this result suggests that transcription and translation of NifA are not affected in LC12 and LC24, unless the presence of *nifA* rather than *lacZ* sequences downstream from the translational start site causes an increase in transcription or translation in the *snoA* or *snoC* mutants.

**Half-life of NifA protein.** To compare the rates of NifA

synthesis and degradation in MC1061 and the *sno* mutants, we pulse-labeled aerated log-phase cells for 2 min and monitored the decline of labeled NifA. Since the half-life of NifA-AUG1 appeared to be shorter than 2 min, making reliable measurement difficult (data not shown), we measured the half-life of the more stable NifA- $\Delta$ N (Fig. 6 and 7; Table 3). Although the activity of NifA- $\Delta$ N was increased only slightly by the *lon*, *snoB*, or *snoC* mutations, these mutations did affect the accumulation of NifA- $\Delta$ N and NifA-AUG1 under 21% oxygen in a similar way. We found that, as expected, the half-life of NifA- $\Delta$ N was increased in the *lon* mutant HA62 from about 3.5 h to about 7 h (Table 3). The *snoB* insertion by itself had no significant effect on the half-life of NifA- $\Delta$ N, consistent with the failure of this mutation to increase accumulation of NifA- $\Delta$ N. Also in accordance with the results from the Western analysis, NifA- $\Delta$ N expressed in a *snoB lon* double mutant showed an increase in half-life that was greater than the effect of the *lon* mutation alone, to about 21 h (Table 3). The half-life of NifA- $\Delta$ N in LC24 (*snoC*) and in HA64 (*lon snoC*) could not be accurately assessed because the data points were more widely scattered for these two strains (Fig. 7; Table 3).

## DISCUSSION

Previous work has shown that the transcriptional activity of *R. meliloti* NifA expressed from a constitutive promoter in either *R. meliloti* or *E. coli* is much lower when cells are grown under aerobic conditions rather than microaerobic conditions (2, 15). This decline in NifA activity with increasing oxygen is partially due to a decline in the steady-state level of NifA and partially due to a decrease in specific activity (15). We set out to identify factors in *E. coli* that mediate the decrease in NifA activity at high oxygen, either by decreasing NifA accumulation or by contributing to the inactivation of NifA. Our selection scheme made use of a NifA-regulated promoter (*R. meliloti nifH*) fused to *lacZ*, which permits the growth of cells on lactose minimal medium in the presence of active NifA. Of the three classes of *E. coli* mutants identified by this method, *snoA* (*lon*) and *snoC* significantly altered the degradation rate of NifA, whereas *snoB* increased accumulation of NifA only slightly

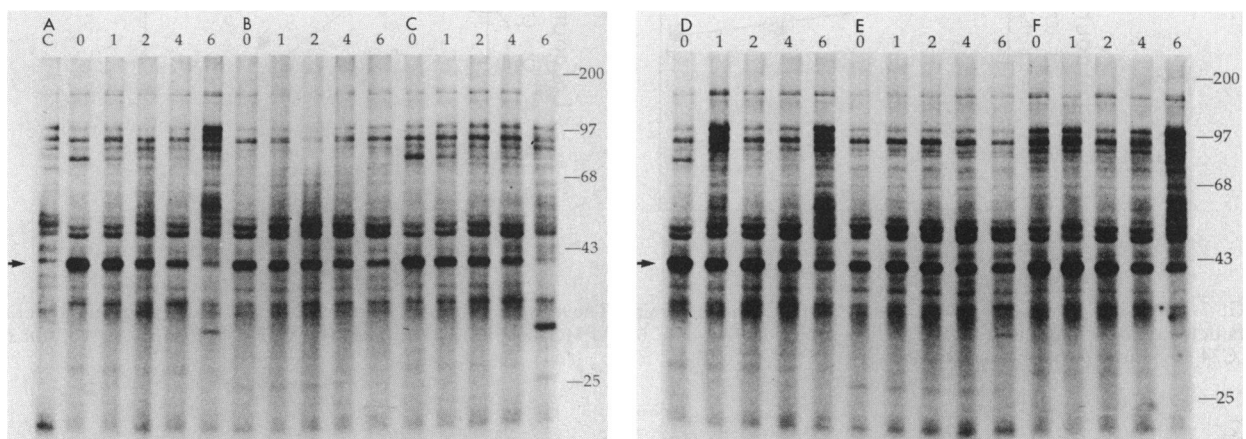


FIG. 6. Stability of NifA in *E. coli* MC1061 and mutant derivatives: SDS-polyacrylamide gel electrophoresis of immunoprecipitated NifA after a 2-min pulse with [ $^{35}$ S]methionine and a chase of 0 to 6 h with excess unlabeled methionine. The length of the chase for each lane is indicated in hours at the top of the figure. Lane C contained MC1061 without pEH $\Delta$ RI (no NifA- $\Delta$ N). (A) MC1061 with pEH $\Delta$ RI; (B) HA62 (*lon*) with pEH $\Delta$ RI; (C) LC23 (*snoB*) with pEH $\Delta$ RI; (D) LC24 (*snoC*) with pEH $\Delta$ RI; (E) HA63 (*lon snoB*) with pEH $\Delta$ RI; (F) HA64 (*lon snoC*) with pEH $\Delta$ RI. Positions of molecular weight markers (in thousands) are shown on the right.

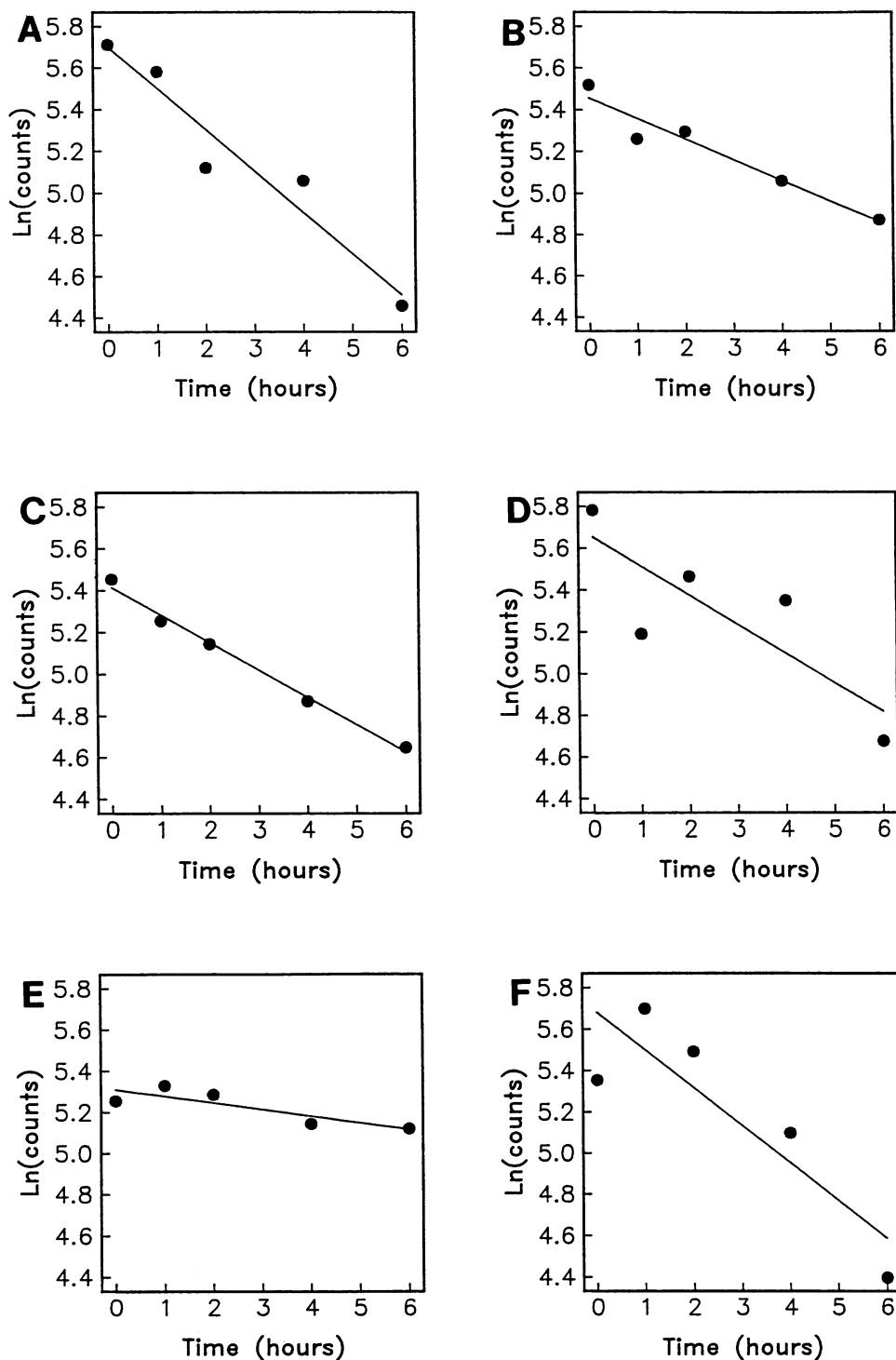


FIG. 7. Half-life of NifA- $\Delta$ N in *E. coli* wild-type and mutant strains. The amount of NifA is given as the natural log of the number of decay events detected over 1,000 min for each NifA band visible in Fig. 6. (A) MC1061; (B) HA62 (*lon*); (C) LC23 (*snoB*); (D) HA63 (*lon snoB*); (E) LC24 (*snoC*); (F) HA64 (*lon snoC*).

yet still caused an increase in NifA activity equivalent to that of *lon* or *snoC* and may therefore exert an effect on the rate of NifA inactivation under aerobic growth conditions.

***snoA* (*lon*) and *snoC* mutations decrease NifA degradation.** Previous results have shown that inactivation of NifA at high

oxygen levels in *E. coli* and *R. meliloti* is not due solely to proteolysis, since for some mutant forms of NifA such as NifA- $\Delta$ N the level of NifA in the cell declines only slightly as oxygen is increased, whereas NifA activity decreases much more rapidly (15). This lack of correspondence between

TABLE 3. Half-life of NifA-ΔN in MC1061 and *sno* mutants at 28°C<sup>a</sup>

Strain	Half-life (h) <sup>b</sup>	Range (h)
MC1061	3.5	2.7–5.0
HA62 ( <i>lon</i> )	7.0	5.4–10.0
LC23 ( <i>snoB</i> )	5.3	4.8–5.9
LC24 ( <i>snoC</i> )	5.0	2.8–24.5
HA63 ( <i>lon snoB</i> )	21.4	12.6–70.2
HA64 ( <i>lon snoC</i> )	3.8	2.3–10.3

<sup>a</sup> Half-lives were calculated by a least-squares fit to an exponential decay curve for a single experiment. The range represents the 95% confidence level (2 standard deviations from the mean slope). Another experiment produced similar results (data not shown).

<sup>b</sup> Data are from the pulse-chase experiment shown in Fig. 6 and 7.

NifA levels and NifA activity is probably due to increased stability of oxygen-inactivated NifA-ΔN relative to NifA-AUG1, as previously discussed (15). Here we have found that a mutation in *lon* appears to substantially lessen the rate of degradation of NifA-AUG1 under 21% oxygen (Fig. 1), while having a much smaller effect on the decline in NifA-AUG1 activity with increasing oxygen (Table 2). The resulting discrepancy between NifA-AUG1 accumulation and activity is similar to that previously seen for NifA-ΔN and might be explained by the accumulation of an inactive form of NifA under 21% oxygen in both cases. Since the *lon* and *snoC* mutations increase NifA activity as well as accumulation under 21% oxygen, it is likely that degradation of both active and inactive forms of NifA under 21% oxygen is decreased relative to that of wild-type *E. coli*, resulting in increased accumulation of both active and inactive forms of NifA. A less likely possibility is that *lon* and *snoC* degrade only inactive NifA and affect the level of active NifA indirectly by eliminating the pool of inactive NifA and consequently preventing the reversal of NifA inactivation. However, since the inactivation of the similarly oxygen-sensitive NifA from *Bradyrhizobium japonicum* is irreversible (17), this is unlikely to be correct.

*E. coli* containing both the *lon* and *snoC* mutations shows no additional increase in NifA accumulation or half-life when compared with a strain containing only a *lon* mutation. If the products of the *lon* and *snoC* genes were independent proteases, each capable of degrading NifA in the absence of the other, the effects of the two mutations should be additive. Since this is not the case, the products of the *lon* and *snoC* genes must work cooperatively to degrade NifA. The idea that the *lon* product may require another *E. coli* factor to degrade some proteins such as SulA, an unstable regulator of cell division, has been suggested (27).

A *snoB* mutation may increase aerobic NifA activity. In contrast to mutations in *lon* and *snoC*, a mutation in *snoB* increases NifA activity 10-fold while causing only a slight increase in NifA accumulation. One possible explanation is that the *snoB* mutation specifically prevents the degradation of an active form of NifA. If active NifA makes up a small fraction of total NifA under 21% oxygen, a 10-fold increase in accumulation of only the active form of NifA might not significantly increase the amount of total NifA visible on a Western blot. Alternatively, the effect of the *snoB* mutation may be primarily on the specific activity of NifA, rather than on its accumulation. The decline in NifA activity without a concomitant decline in NifA accumulation with increasing oxygen (15) (Table 2; Fig. 1 through 4) confirms that inactivation of NifA can occur by a mechanism other than

degradation. Inactivation of NifA by oxygen has been proposed to occur through a change in the oxidation state of a bound metal ion (12, 13) or through the oxidation of intermolecular or intramolecular disulfide bridges (12). This model for NifA inactivation by oxygen does not immediately suggest the involvement of host factors in the process. However, it is possible that insertions in *snoB* could indirectly protect NifA from oxidative damage, for example, by causing an increase in the level of enzymes such as superoxide dismutase and catalase, which protect the cell from oxidative damage. Alternatively, the *snoB* product could act directly to decrease NifA activity in the presence of oxygen, suggesting a role as functional analog of *K. pneumoniae* NifL.

In light of the failure of a *snoB* mutation to significantly increase the accumulation of NifA, the large increase in NifA accumulation in a *snoB lon* double mutant relative to accumulation in a *lon* mutant was unexpected. It is possible that the *snoB* product increases the susceptibility of NifA to degradation by a Lon-independent pathway or degrades NifA directly. If this is true, the absence of a significant increase in NifA accumulation in a *snoB* mutant might be due to a compensating increase in Lon-mediated degradation, masking the effect of the *snoB* mutation of NifA accumulation.

**Regulation of NifA in a heterologous system.** The activity of *R. meliloti* NifA declines as oxygen is increased in both *E. coli* and *R. meliloti* for all NifA mutants tested (3, 15), suggesting that the mechanisms through which oxygen affects NifA activity in these two organisms are likely to have some similarities. However, posttranscriptional regulation of NifA in *E. coli* and *R. meliloti* differs in some respects. In *E. coli*, NifA-AUG1 accumulates to a very low level, whereas mutated forms of NifA in which the amino-terminal domain of NifA has been altered accumulate to much higher levels. In contrast, in *R. meliloti* small alterations of the NifA amino-terminal domain have little or no effect, whereas deletion of this domain decreases NifA accumulation (15). Until further experiments are carried out in *R. meliloti*, the relevance of our experiments in the heterologous *E. coli* system to the normal regulation of NifA by oxygen will remain unclear. However, these experiments point out a possible approach for the study of NifA regulation in *R. meliloti*. In addition, elucidation of the role of *snoB* and *snoC* in the degradation of native *E. coli* proteins will provide insight into the control of protein stability in *E. coli*.

#### ACKNOWLEDGMENTS

We thank Lisa Albright for many valuable discussions and Georg Jander for his help with the mutant selection technique.

This work was supported by a grant from Hoechst AG to Massachusetts General Hospital.

#### REFERENCES

- Berg, D. 1977. Insertion and excision of the transposable kanamycin resistance determinant Tn5, p. 205–212. In A. I. Bukhari, J. A. Shapiro, and S. L. Adhya (ed.), DNA insertion elements, plasmids, and episomes. Cold Spring Harbor Laboratory, Cold Spring Harbor, N.Y.
- Better, M., G. Ditta, and D. R. Helinski. 1985. Deletion analysis of *Rhizobium meliloti* symbiotic promoters. EMBO J. 4:2419–2424.
- Beynon, J. L., M. K. Williams, and F. C. Cannon. 1988. Expression and functional analysis of the *Rhizobium meliloti* *nifA* gene. EMBO J. 7:7–14.
- Blake, M. S., K. H. Johnston, G. J. Russell-Jones, and E. C. Gotschlich. 1984. A rapid, sensitive method for detection of



- alkaline phosphatase-conjugated anti-antibody on Western blots. *Anal. Biochem.* **136**:175-179.
5. Boyd, D., C.-D. Guan, S. Willard, W. Wright, K. Strauch, and J. Beckwith. 1987. Enzymatic activity of alkaline phosphatase precursor depends on its cellular location, p. 89-93. In A. Torriani-Gorini, F. G. Rothman, S. Silver, A. Wright, and E. Yagil (ed.), *Phosphate metabolism and cellular regulation in microorganisms*. American Society for Microbiology, Washington, D.C.
  6. Casadaban, M. J., and S. N. Cohen. 1980. Analysis of gene control signals by DNA fusion and cloning in *Escherichia coli*. *J. Mol. Biol.* **138**:179-207.
  7. Chin, D. T., S. A. Goff, T. Webster, T. Smith, and A. E. Goldberg. 1988. Sequence of the *lon* gene in *Escherichia coli*. *J. Biol. Chem.* **263**:11718-11728.
  8. Chomczynski, P., and P. K. Qasba. 1984. Alkaline transfer of DNA to plastic membrane. *Biochem. Biophys. Res. Commun.* **122**:340-344.
  9. David, M., M.-L. Daveran, J. Batut, A. Dedieu, O. Domergue, J. Ghai, C. Hertig, P. Boistard, and D. Kahn. 1988. Cascade regulation of *nif* gene expression in *Rhizobium meliloti*. *Cell* **54**:671-683.
  10. Deutch, C. E., and R. L. Soffer. 1978. *Escherichia coli* mutants defective in dipeptidyl carboxypeptidase. *Proc. Natl. Acad. Sci. USA* **75**:5998-6001.
  11. Ditta, G., E. Virts, A. Palomares, and C. H. Kim. 1987. The *nifA* gene of *Rhizobium meliloti* is oxygen regulated. *J. Bacteriol.* **169**:3217-3223.
  12. Fischer, H.-M., T. Bruderer, and H. Hennecke. 1988. Essential and non-essential domains in the *Bradyrhizobium japonicum* NifA protein: identification of indispensable cysteine residues potentially involved in redox reactivity and/or metal binding. *Nucleic Acids Res.* **16**:2207-2224.
  13. Fischer, H.-M., S. Fritsche, B. Herzog, and H. Hennecke. 1989. Critical spacing between two essential cysteine residues in the interdomain linker of the *Bradyrhizobium japonicum* NifA protein. *FEBS Lett.* **255**:167-171.
  14. Fischer, H.-M., and H. Hennecke. 1987. Direct response of *Bradyrhizobium japonicum* *nifA*-mediated *nif* gene regulation to cellular oxygen status. *Mol. Gen. Genet.* **209**:621-626.
  15. Huala, E., and F. M. Ausubel. 1989. The central domain of *Rhizobium meliloti* NifA is sufficient to activate transcription from the *R. meliloti* *nifH* promoter. *J. Bacteriol.* **171**:3354-3365.
  16. Kohara, Y., K. Akiyama, and K. Isono. 1987. The physical map of the whole *E. coli* chromosome: application of a new strategy for rapid analysis and sorting of a large genomic library. *Cell* **50**:495-508.
  17. Kullik, I., H. Hennecke, and H. M. Fischer. 1989. Inhibition of *Bradyrhizobium japonicum* *nifA*-dependent *nif* gene activation by oxygen occurs at the NifA protein level and is irreversible. *Arch. Microbiol.* **151**:191-197.
  18. Levinson, A., D. Silver, and B. Seed. 1984. Minimal size plasmids containing an M13 origin for production of single-strand transducing particles. *J. Mol. Appl. Genet.* **2**:507-517.
  19. Meade, H. M., S. R. Long, G. B. Ruvkun, S. E. Brown, and F. M. Ausubel. 1982. Physical and genetic characterization of symbiotic and auxotrophic mutants of *Rhizobium meliloti* induced by transposon Tn5 mutagenesis. *J. Bacteriol.* **149**:114-122.
  20. Miller, J. H. 1972. *Experiments in molecular genetics*. Cold Spring Harbor Laboratory, Cold Spring Harbor, N.Y.
  21. Parsell, D. A., and R. T. Sauer. 1989. The structural stability of a protein is an important determinant of its proteolytic susceptibility in *Escherichia coli*. *J. Biol. Chem.* **264**:7590-7595.
  22. Putney, S. D., N. J. Royal, H. N. De Vegvar, W. C. Herlihy, K. Biemann, and P. Schimmel. 1981. Primary structure of a large aminoacyl-tRNA synthetase. *Science* **213**:1497-1501.
  23. Ronson, C. W., B. T. Nixon, L. M. Albright, and F. M. Ausubel. 1987. *Rhizobium meliloti* *ntfA* (*rpoN*) gene is required for diverse metabolic functions. *J. Bacteriol.* **169**:2424-2431.
  24. Ruvkun, G. B., and F. M. Ausubel. 1981. A general method for site-directed mutagenesis in prokaryotes. *Nature (London)* **289**:85-88.
  25. Sanger, F., S. Nicklen, and A. R. Coulson. 1977. DNA sequencing with chain-terminating inhibitors. *Proc. Natl. Acad. Sci. USA* **74**:5463-5467.
  26. Sasaki, I., and G. Bertani. 1965. Growth abnormalities in Hfr derivatives of *Escherichia coli* strain C. *J. Gen. Microbiol.* **40**:365-376.
  27. Schoemaker, J. M., R. C. Gayda, and A. Markovitz. 1984. Regulation of cell division in *Escherichia coli*: SOS induction and cellular location of the Sula protein, a key to *lon*-associated filamentation and death. *J. Bacteriol.* **158**:551-561.
  28. Singer, M., T. A. Baker, G. Schnitzler, S. M. Deischel, M. Goel, W. Dove, K. J. Jaacks, A. Grossman, J. W. Erickson, and C. A. Gross. 1989. A collection of strains containing genetically linked alternating antibiotic resistance elements for genetic mapping of *Escherichia coli*. *Microbiol. Rev.* **53**:1-24.
  29. Storz, G., F. S. Jacobson, L. A. Tartaglia, R. W. Morgan, L. A. Silveira, and B. N. Ames. 1989. An alkyl hydroperoxide reductase induced by oxidative stress in *Salmonella typhimurium* and *Escherichia coli*: genetic characterization and cloning of *ahp*. *J. Bacteriol.* **171**:2049-2055.
  30. Wanner, B. L. 1986. Novel regulatory mutants of the phosphate regulon in *Escherichia coli* K-12. *J. Mol. Biol.* **191**:39-58.